ALDH1A1 activity in tumor-initiating cells remodels myeloid-derived suppressor cells to promote breast cancer progression

Cuicui Liu[1,9], Jiankun Qiang[1], Qiaodan Deng[1], Jie Xia[1], Lu Deng[2], Lei Zhou[3], Dong Wang[4], Xueyan He[1], Ying Liu[5], Botao Zhao[5], Jinhui Lv[6], Zuoren Yu[6], Qun-Ying Lei[1], Zhi-Ming Shao[1,7,*], Xiao-Yong Zhang[5,8,*], Lixing Zhang[1,*], Suling Liu[1,9,*]

[1] Fudan University Shanghai Cancer Center & Institutes of Biomedical Sciences; Cancer Institutes; Key Laboratory of Breast Cancer in Shanghai; The Shanghai Key Laboratory of Medical Epigenetics; Shanghai Key Laboratory of Radiation Oncology; The International Co-laboratory of Medical Epigenetics and Metabolism, Ministry of Science and Technology; Shanghai Medical College; Fudan University, Shanghai 200032, China.

[2] Stowers Institute for Medical Research, 1000 E 50 St, Kansas, MO 64110, USA.

[3] Institute of Pathology and Southwest Cancer Center, Southwest Hospital, Third Military Medical University (Army Medical University), Chongqing 400038, China.

[4] WPI Nano Life Science Institute (WPI-NanoLSI), Kanazawa University, Kakuma-machi, Kanazawa 920-1192, Japan.

[5] Institute of Science and Technology for Brain-Inspired Intelligence, Fudan University, Shanghai 200433, China.

[6] Research Center for Translational Medicine, Shanghai East Hospital, Tongji University School of Medicine, Shanghai, 200120, China.

[7] Department of Breast Surgery, Precision Cancer Medicine Center, Fudan University Shanghai Cancer Center, Shanghai 200032, China.

[8] Key Laboratory of Computational Neuroscience and Brain-Inspired Intelligence (Fudan University), Ministry of Education, Shanghai 200433, China.

[9] Jiangsu Key Lab of Cancer Biomarkers, Prevention and Treatment, Collaborative Innovation Center for Cancer Medicine, Nanjing Medical University, Nanjing 211166, China

*Corresponding authors:

Suling Liu, Fudan University Shanghai Cancer Center, Key Laboratory of Breast Cancer in Shanghai, Cancer Institutes, Shanghai 200032, China; Tel/Fax: 086-21-34774409. Email: suling@fudan.edu.cn

Lixing Zhang, Fudan University Shanghai Cancer Center, Key Laboratory of Breast Cancer in Shanghai, Cancer Institutes, Shanghai 200032, China; Tel/Fax: 086-21-34771071. Email: zhang_lx@fudan.edu.cn

Xiao-Yong Zhang, Institute of Science and Technology for Brain-Inspired Intelligence, Fudan University, Shanghai 200433, China. Email: xiaoyong_zhang@fudan.edu.cn

Zhi-Ming Shao, Department of Breast Surgery, Precision Cancer Medicine Center, Fudan University Shanghai Cancer Center, Shanghai 200032, China; Tel/Fax: 086-21-64175590. Email: zhimingshao@yahoo.com

Supplementary Materials and methods

Co-culture of Bone marrow cells and 4T1 cells

Bone marrow cells (BMCs) were harvested from naive female Balb/c mice and contactless co-cultured with 4T1 cells in six-well plates (1-2 $\times 10^5$cells/well) for a total of 6 days. Bone marrow cells were cultured in the bottom of a six-well dishes with 24 mm Transwell inserts with a 0.4 μm pore size on top (Corning Life Sciences, USA). In the Transwell insert, 1×10^4 4T1 cells were plated on day 0. Transwell inserts were discarded on day 3 and a fresh insert with 1×10^4 corresponding 4T1 cells was added again. On day 7, bone marrow cells were stained with CD45, Gr1 and CD11b, and percentage of $Gr1^+CD11b^+$MDSCs were analyzed by flow cytometry. All experiments were repeated more than 3 times.

MDSC depletion

MDSCs were depleted with anti-Ly6G antibody (200ug/mouse, clone1A8; BioXCell, USA) in vivo. Anti-Ly6G antibody and isotype control antibody (200 μg/mouse, IgG, Sigma-Aldrich, USA) were administered intraperitoneally into tumor bearing mice every three days starting from day 3 for a total of six times.

ELISA and Western Blotting

An enzyme linked immunosorbent assay (ELISA) was performed with cell culture supernatants to determine GM-CSF levels, following manufacturer's recommendations (Proteintech^{TM}, USA), and GM-CSF levels were calculated according to the standard curve. For Western Blots, total protein in cells was extracted and boiled in SDS loading buffer, then protein lysates were separated by 10% SDS-PAGE, transferred onto a PVDF membrane and probed with specific primary antibodies. The detailed information about antibodies were shown in Table S1. HRP substrate (Millipore, USA) was used to detect HRP-conjugated secondary with an Image Quant LAS 4000 mini-imaging system (GE, Fairfield, USA). All experiments were repeated more than 3 times.

Mammosphere formation assay

Tumor cells were cultured with MammoCult Human Medium Kit (STEMCELL, USA) supplemented with 4 μg/mL Heparin (STEMCELL), 1 μg/mL hydrocortisone (Sigma-Aldrich), and 1% pen-strep antibiotic (Beyotime, China). 100 or 1000 tumor cells in 100ul medium were plated in each well of 96-well ultra-low attachment plates (Corning Life Sciences) and cultured for about 2 weeks. Fresh complete MammoCult medium was added every 3 days. Sphere number were counted and photographed for further statistical analysis. The same operation procedure was performed in 6-well ultralow attachment plates. After the culture was completed, spheres were digested into single-cell suspensions with 0.25% trypsin for subsequent experiments.

HPLC-MS

Samples were vortex mixed for 2 minutes, settled for several minutes, and then 1ml cold70% methanol solution was added and samples were vortexed for 3 minutes. Samples were soaked in liquid nitrogen for 2 minutes, and then defrosted on ice for 5 minutes and vortexed for 2 minutes, repeat the above operation once again. Samples were added 300ul extracting reagent containing internal standard 2-chlorophenylalanine (1 μg/ml), and splintered cells with ultrasonic on ice for 5minutes. Then, samples were centrifuged at 4℃ for 5 minutes at 12,000 rpm/min. Supernatants were placed in a new 1.5 ml tube. 100μL of supernatant was used for UPLC-MS/MS. Ultraperformance liquid chromatography, UPLC (Shim-pack UFLC SHIMADZU CBM30A, https://www.shimadzu.com/), tandem mass spectrometry, MS/MS (QTRAP@6500+, https://sciex.com/).

Intracellular pH detection in vitro

BCECF (2′,7′-bis-(2-carboxyethyl) -5-(and-6) -carboxyfluorescein) AM is the most widely used fluorescent indicator for intracellular pH. Cancer cells were seeded in six-well plates and incubated under normal conditions till approximately 70-80% confluency. Prepare viable cells in suspension (~10^6 cells/mL). Dilute an aliquot of 1 mM BCECF AM ester stock solution 100- to 500-fold into a physiological saline buffer such as PBS. Add one volume of aqueous AM ester dispersion to one volume of cell suspension. Incubate for 15–60 minutes at 4℃ to 37℃. Wash the cells twice with fresh culture medium and then detect the fluorescence at 488 nm by flow cytometry. All experiments were repeated more than 3 times.

pH_{enh} imaging with MRI in vivo

Control, Aldh1a1 or K193Q/R mutant 4T1 ($5x10^4$) cells were transplanted orthotopically into Balb/c mice respectively. After 18 days, tumors volumes were about 500 mm^3, tumor-bearing mice were imaged by Bruker BioSpec 11.7T horizontal MR scanner with a 75/40 mm diameter quadrature volume coil. The mice were kept anesthetized by a gas mixture of

isoflurane/oxygen (2%/98%, volume ratio). Bite and ear bars were used to reduce respiration-induced motion artifacts, and the respiration and rectal temperature were monitored (SA Instruments, Inc., Stony Brook, NY, USA) during imaging. After a Localizer scanning for animal positioning, respiration-gated T2-weighted imaging were achieved using a rapid acquisition with relaxation enhancement sequence. For CEST-MRI, a continuous wave (CW)-MT sequence with a saturation pulse power of 0.6μT and 1.1 μT was used. Z-spectra, presented as measured signals (S_{sat}) normalized by a reference signal (S_0), were acquired with RF offsets from -2500 to 2500 Hz with a step width of 50 Hz (-5 to 5 ppm on 11.7 T). S_0 was obtained by setting the RF offset to 100000 Hz (20 ppm on 11.7 T) for signal normalization. MRI data was processed using MATLAB R2018a software (MathWorks, Natick, MA, USA). The enhancement of pH sensitivity was obtained by combining both amide- and guanidyl-CEST images, and subtracting them.

Supplementary Figures and Legends

Supplementary Fig. S1

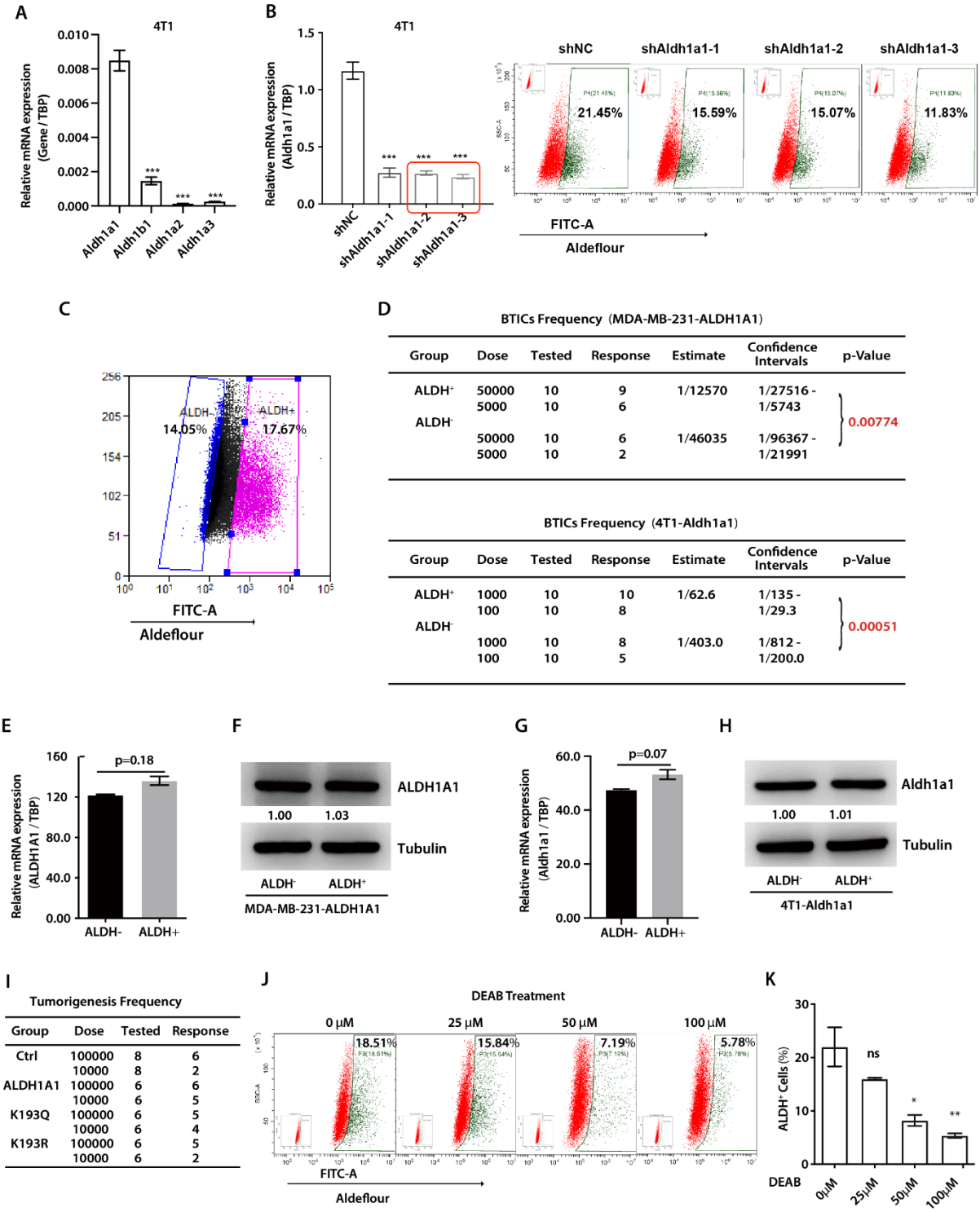

Fig. S1. ALDH1A1 increased ALDH$^+$ BTICs and promoted breast tumor progression relying on its enzyme activity.

(A) The mRNA expression of Aldh1a1, Aldh1a2, Aldh1a3 and Aldh1b1 in 4T1 cells were quantified by qRT-PCR. **(B)** Aldh1a1 knockdown (shAldh1a1) in 4T1 significantly decreased ALDH enzyme activity. The knockdown efficiency of Aldh1a1 in 4T1 was verified by qRT-PCR. **(C)** $ALDH^-$ and $ALDH^+$ cells were sorted using the flow cytometry based on their different ALDH enzyme activity in ALDH1A1-MDA-MB-231 and Aldh1a1-4T1 BC cells. **(D)** $ALDH^+$ cancer cells had more tumorigenic ability in comparison to the $ALDH^-$ ones. The grafted tumor assay was performed using serial dilutions with sorted $ALDH^-$ and $ALDH^+$ MDA-MB-231-ALDH1A1 cells ($5x10^4$, $5x10^3$ cells/fat pad) or sorted $ALDH^-$ and $ALDH^+$ 4T1- Aldh1a1 cells (1000, 100 cells/fat pad) into female nude mice and Balb/c mice respectively. Tumorigenesis was determined after 4 weeks for MDA-MB-231 cells and 4T1 cells. The BTIC frequency in tumors was calculated by the LDA. **(E-H)** The ALDH1A1/Aldh1a1 protein and mRNA expression were equal between ALDH- cells and ALDH+ cells. ALDH1A1/Aldh1a1 mRNA expression was quantified by qRT-PCR and ALDH1A1/Aldh1a1 protein was measured by Western Blots. **(I)** The xenografted tumor assay was performed using serial dilutions ($1x10^5$, $1x10^4$ cells/fat pad) with ALDH1A1 or K193Q/R mutant MDA-MB-231 cells. Tumorigenesis was determined after 4 weeks. **(J, K)** 4T1 cells were treated with the indicated concentrations of DEAB for 48 hours; the percentage of $ALDH^+$ BTIC population was subsequently decreased.

Data were presented as mean ± SEM, unpaired t test was utilized for **E** and **G**, one or two-way ANOVA test was utilized for other figures; ns, no significance, $**p < 0.01$, $***p < 0.001$.

Supplementary Fig. S2

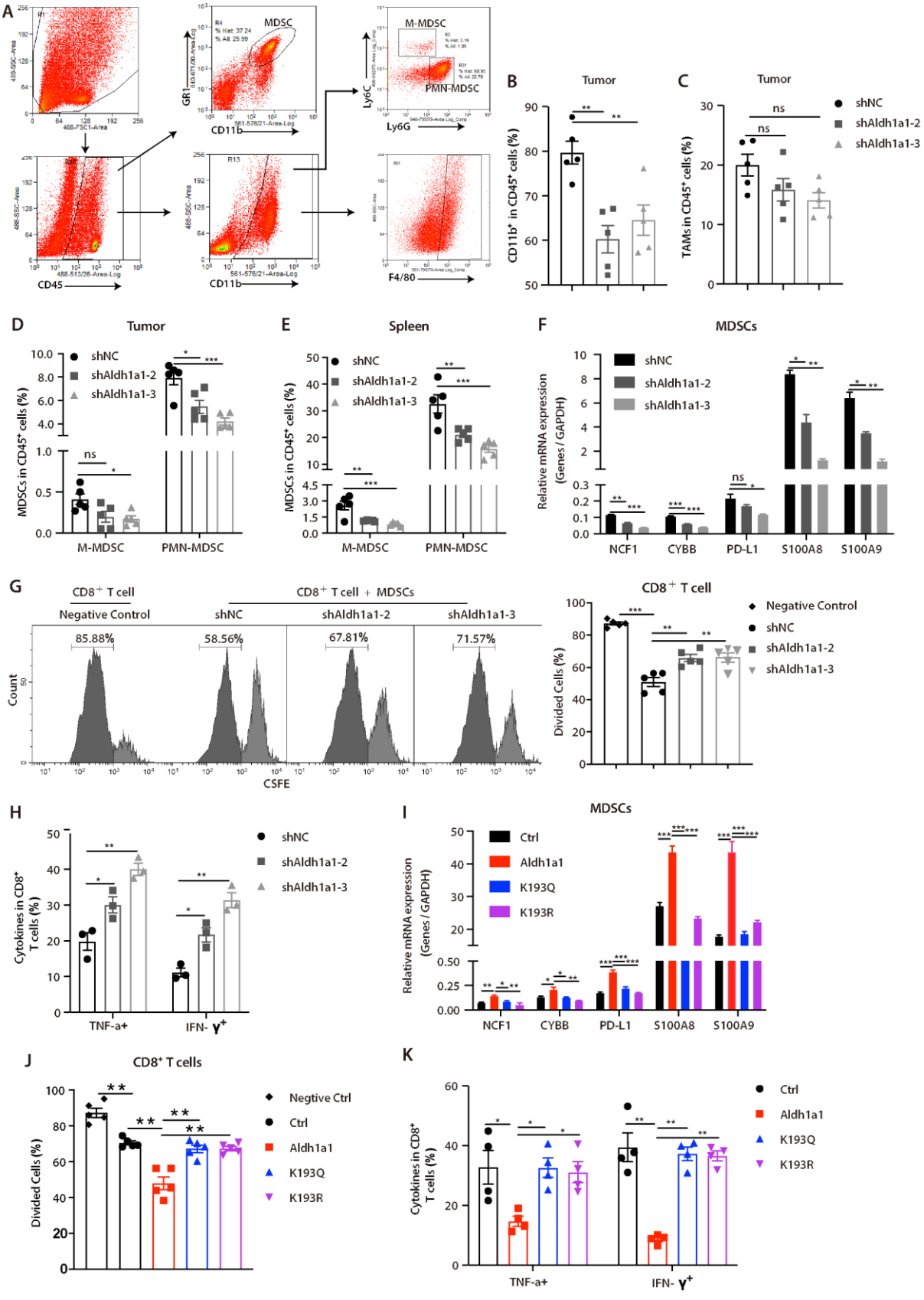

136

137 **Fig. S2. Aldh1a1 increased MDSC enrichment as well as its immunosuppressive function.**

(A) Gating strategy for the analysis of MDSCs and TAMs by flow cytometry. Proportion (in $CD45^+$ cells) of MDSCs from tumors and host spleens were analyzed with surface markers CD11b and Gr1. $CD45^+CD11b^+Ly6C^{high}Ly6G^-$ for M-MDSCs, $CD45^+CD11b^+Ly6C^{low}Ly6G^+$ for PMN-MDSCs and $CD45^+CD11b^+F4/80^+$ for TAMs. **(B)** Percentage of $CD11b^+$ myeloid cells from shNC- and shAldh1a1-4T1 tumors (n=5 /group). **(C)** Proportion (in $CD45^+$ cells) of TAMs from shNC- and shAldh1a1-4T1 tumors (n=5 /group). **(D, E)** Proportion (in $CD45^+$ cells) of M-MDSCs and PMN-MDSCs in the tumors and host spleens from shNC- and shAldh1a1-4T1 mice (n=5 /group). **(F)** qRT-PCR analysis of the expression of NCF1, CYBB, PD-L1, S100A8 and S100A9 in MDSCs derived from shNC- and shAldh1a1-4T1 tumors (n=3 /group). **(G)** $CD8^+$ T cells were isolated from wild-type Balb/c mice and stimulated with cocktail. These $CD8^+$ T cells were co-cultured in vitro with MDSCs derived from shNC- and shAldh1a1-4T1 tumors, and the proliferation of T cells was analyzed with CSFE assay (n=5 /group). **(H)** The proportion IFN-γ^+ $CD8^+$ T cells and TNF-α^+ $CD8^+$ T cells in co-culture between MDSCs and activated $CD8^+$ T cells in vitro (n=3 /group). **(I)** qRT-PCR analysis of the expression of NCF1, CYBB, PD-L1, S100A8 and S100A9 in MDSCs derived from Ctrl-, Aldh1a1- and K193Q/R-4T1 tumors (n=3 /group). **(J)** The proliferation of $CD8^+$ T cells of co-culture with MDSCs derived from Ctrl-, Aldh1a1- and K193Q/R-4T1 tumors was analyzed with CSFE assay (n=5 /group). **(K)** The activation of $CD8^+$ T cells of co-culture with MDSCs derived from Ctrl-, Aldh1a1- and K193Q/R-4T1 tumors was validated by the proportion of IFN-γ^+ $CD8^+$ T cells and TNF-α^+ $CD8^+$ T cells (n=4 /group). Data were presented as mean ± SEM, one-way ANOVA test was utilized; ns, no significance, *$p < 0.05$, **$p < 0.01$, ***$p < 0.001$.

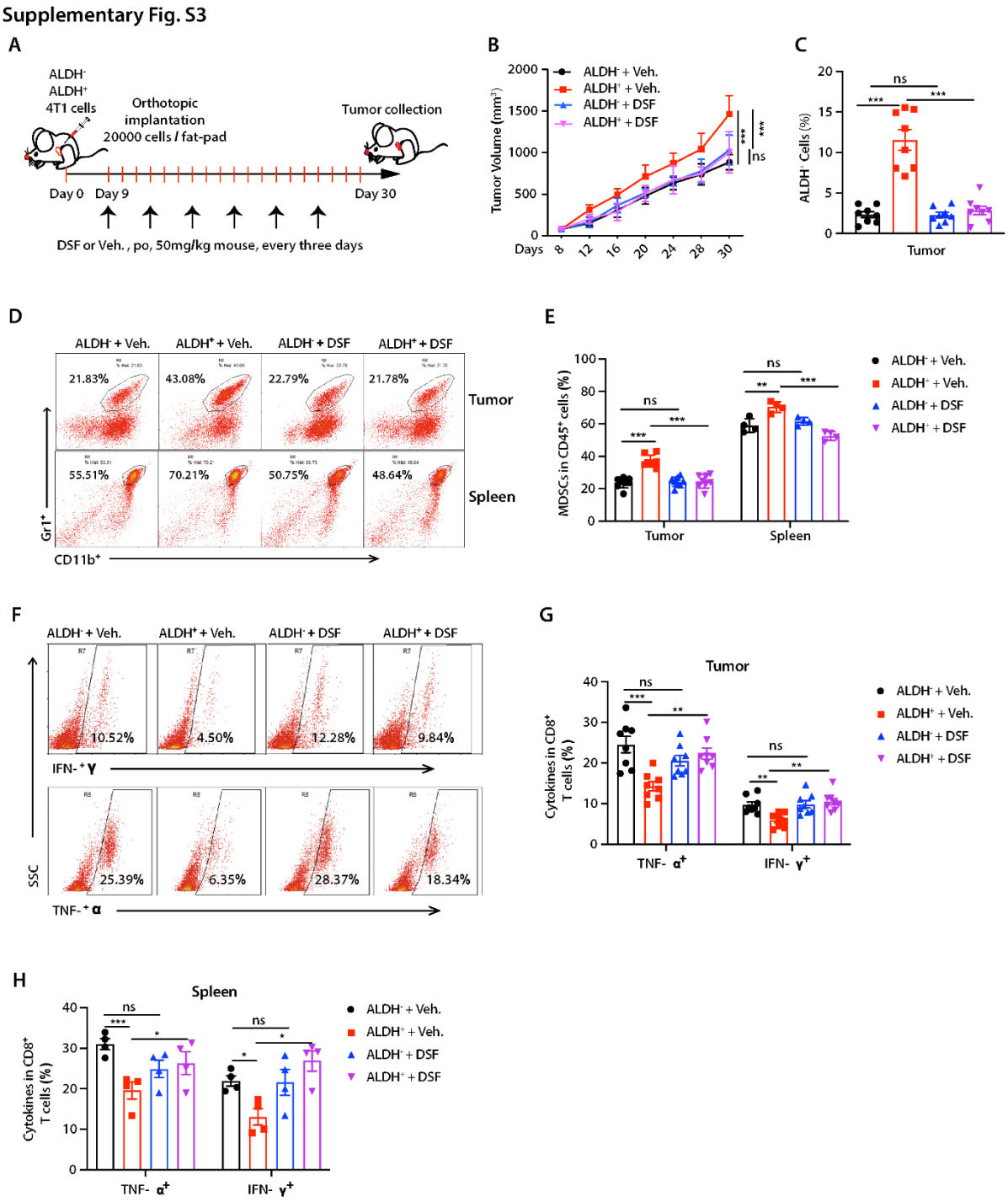

160

161 **Fig. S3. Inhibition of ALDH1A1 enzyme activity reduced MDSC enrichment.**

162 **(A, B)** ALDH$^+$ cancer cells had accelerated tumor growth in comparison to the ALDH$^-$ group,
163 which was blocked by DSF. Sorted ALDH$^-$ and ALDH$^+$ 4T1 cells ($2.5x10^4$/fat pad) were
164 inoculated into female Balb/c mice. After cells inoculated for 3 days, the tumor-bearing mice
165 were treated with DSF (50mg/kg) or vehicle (Veh.) every three days. Tumor growth was

monitored, and tumor volume were measured (n = 8/group). **(C)** DSF significantly reduced $ALDH^+$ BTICs by inhibiting the ALDH enzyme activity. **(D, E)** $Gr1^+CD11b^+$ MDSCs were markedly increased in $ALDH^+$ cell-derived tumors and spleens compared with the $ALDH^-$ cell-derived ones, which was blocked by DSF. Representative flow cytometry dot plots (D) showed $Gr1^+CD11b^+$ $CD45^+$ cells in tumors and spleens of tumor-bearing mice. The percentages (in $CD45^+$ cells) of MDSCs were shown in tumors (n=8/group) and host spleens (n=4/group) (E). **(F-H)** Active $CD8^+$ T cells were also markedly decreased in $ALDH^+$ cell-derived tumors and host spleens compared to the $ALDH^-$ cell-derived ones, which was recovered by DSF. Representative flow cytometry dot plots (F) and proportions of cytokines IFN-γ and TNF-α in $CD8^+$ T cells were shown in tumors (n =8/group) (G) and spleens (H) (n = 4/group). Data were presented as mean ± SEM, one or two-way ANOVA test was utilized; ns, no significance, *$p < 0.05$, **$p < 0.01$, ***$p < 0.001$.

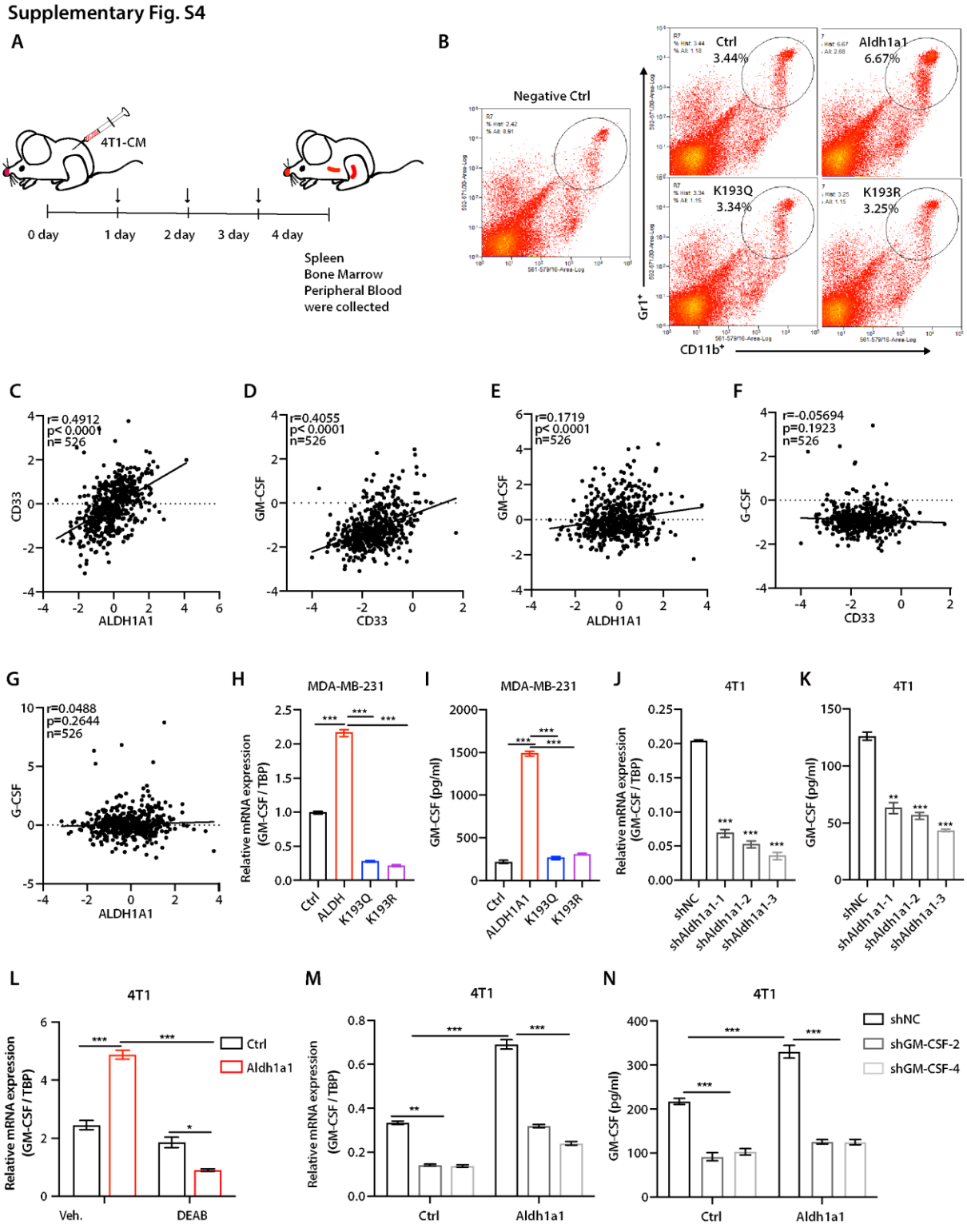

Fig. S4. ALDH1A1 upregulated GM-CSF in BC cells to promote MDSC expansion.

(A) The experimental diagram for MDSCs expansion in vivo induced by conditioned medium. The female Balb/c mice (n=3/group) were injected intradermally with CM derived from control-, Aldh1a1- or K193Q/R-4T1 cells for 3 consecutive days, and the mice were

sacrificed on the fourth day. Aldh1a1-derived CM increased MDSCs in tumor-free Balb/c mice. **(B)** Representative flow cytometry dot plots for $Gr1^{+}CD11b^{+}CD45^{+}$ cells in spleen were shown. **(C-E)** The mRNA expressions of ALDH1A1, CD33 and GM-CSF were positively correlated with each other. Pearson's correlation was calculated. **(F, G)** G-CSF showed no significantly correlation with either CD33 or ALDH1A1 in mRNA levels. **(H, I)** ALDH1A1 upregulated GM-CSF expression. ALDH1A1 and K193Q/R mutant MDA-MB-231 cells were cultured for 24 and 48 hours, respectively. GM-CSF mRNA expression was quantified by qRT-PCR (H) and GM-CSF protein was measured in culture supernatant with ELISA (I). **(J, K)** GM-CSF expression at both mRNA and protein levels were decreased after Aldh1a1-knockdown in 4T1 cells. **(L)** GM-CSF mRNA upregulation induced by active Aldh1a1 was blockaded by DEAB treatment in 4T1 cells. **(M, N)** GM-CSF knockdown (shGM-CSF) efficiency was verified in control and Aldh1a1 4T1 cells. Data were presented as mean ± SEM, one-way ANOVA test was utilized; $^{**}p < 0.01$, $^{***}p < 0.001$.

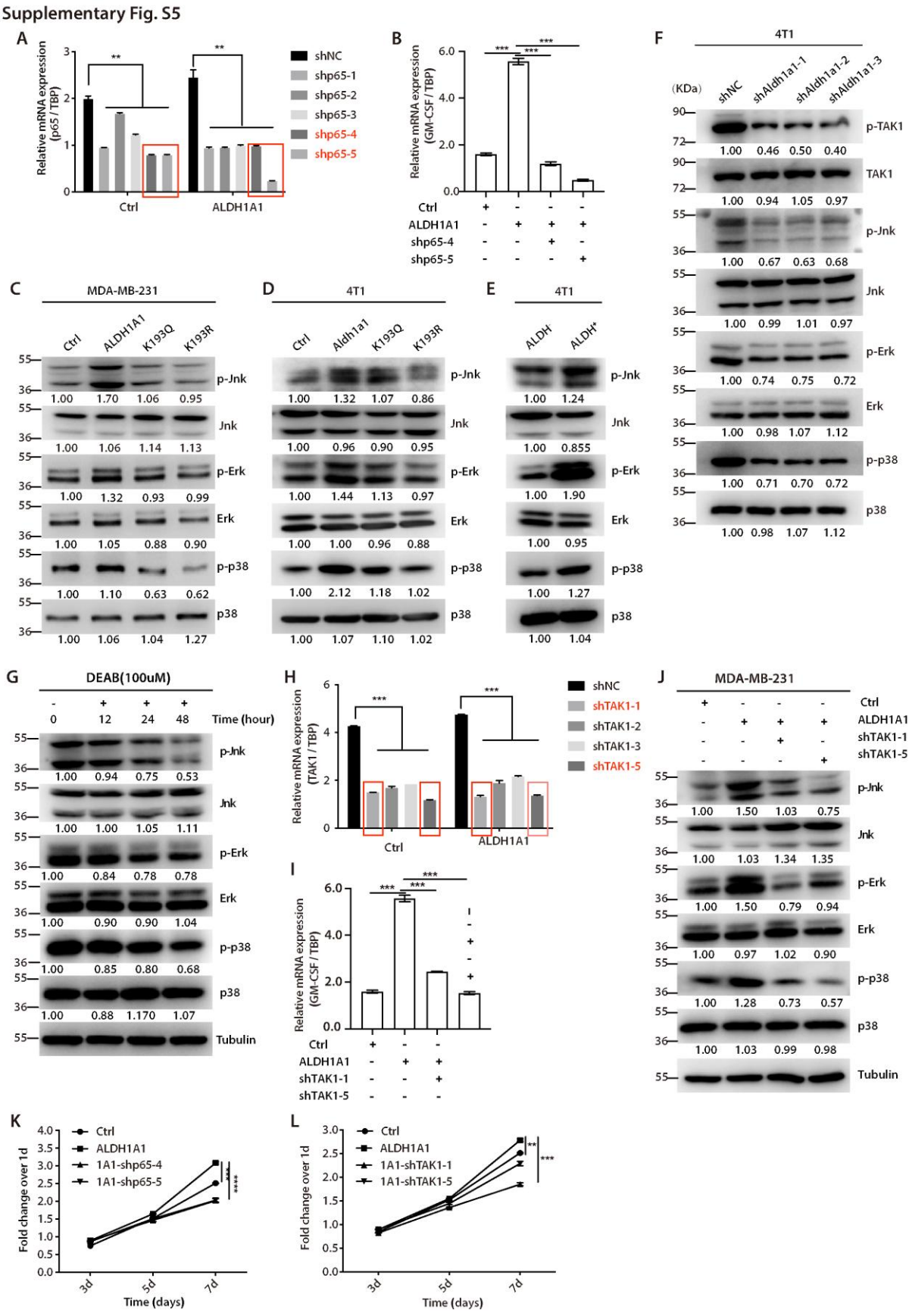

Fig. S5. ALDH1A1, relying on enzyme activity, increased TAK1 phosphorylation to activate MAPK signaling to regulate NFkB pathay.

(A) The knockdown efficiency of p65 (shp65) in control and ALDH1A1 MDA-MB-231 was verified by qRT-PCR. **(B)** GM-CSF mRNA upregulation induced by ALDH1A1 was reversed by p65 knockdown in MDA-MB-231 cells. **(C, D) p-**JNK, p-ERK and p-p38 were increased in ALDH1A1/Aldh1a1 cells, but not K193Q/R mutant cells compared with control in MDA-MB-231 and 4T1 cells analyzed by Western Blot. **(E) p-**JNK, p-ERK and p-p38 were increased in $ALDH^+$ cells analyzed by Western Blot. $ALDH^-$ and $ALDH^+$ cells were sorted from 4T1 cells. **(F)** The expression of p-TAK1, p-JNK, p-ERK and p-p38 were inhibited after Aldh1a1-knockdown in 4T1 cells analyzed by Western Blot. **(G)** DEAB treatment suppressed p-JNK, p-ERK and p-p38 in ALDH1A1 MDA-MB-231 cells analyzed by Western Blot. DEAB treatment (100uM) was applied for different time (0h, 12h, 24h, 48h). **(H)** The knockdown efficiency of TAK1 (shTAK1) in control and ALDH1A1 MDA-MB-231 was verified by qRT-PCR. **(I)** GM-CSF mRNA upregulation induced by ALDH1A1 was reversed by TAK1 knockdown in MDA-MB-231 cells. **(J)** TAK1 knockdown decreased p-JNK, p-ERK and p-p38 upregulated by active ALDH1A1 in MDA-MB-231 cells. **(K, L)** Promoting effect of ALDH1A1 on cell proliferation was reversed by p65 or TAK1 knockdown in MDA-MB-231 ALDH1A1 cells. Data were presented as mean ± SEM, one/two-way ANOVA test was utilized; $^{**}p < 0.01$, $^{***}p < 0.001$.

Supplementary Fig. S6

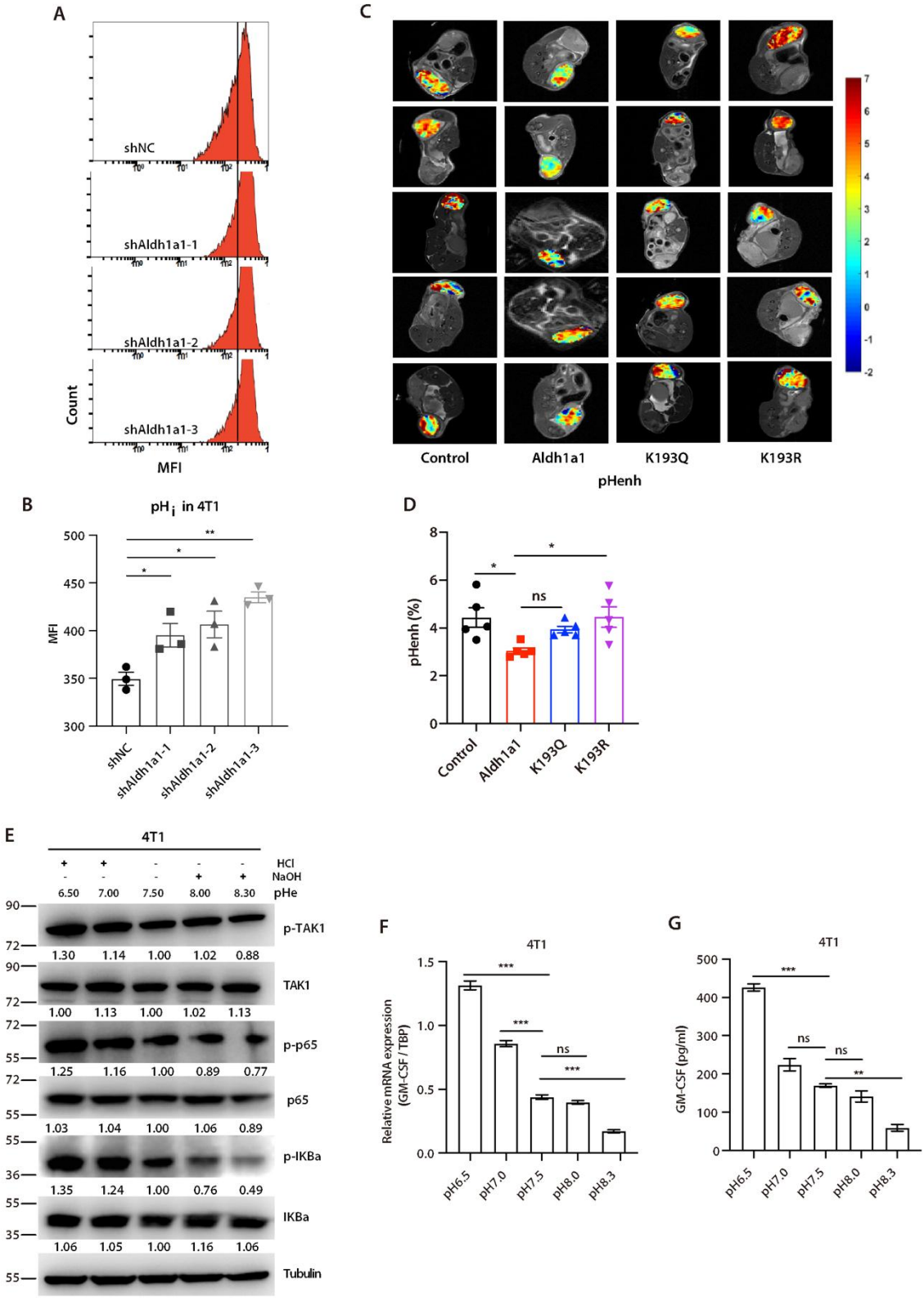

Fig. S6. Aldh1a1 decreased the pH in BC cells to activate TAK1-NFκB pathway and upregulated GM-CSF expression.

(A, B) The results of BCECF-AM fluorescent probe analysis showed that Aldh1a1-knockdown induced the increase of pHi in 4T1 cells. **(C, D)** Control, Aldh1a1 or K193Q/R mutant 4T1 ($5x10^4$) cells were transplanted orthotopically into Balb/c mice respectively. After 18 days, when the average tumor volume in Aldh1a1 group was about 500 mm^3, tumor-bearing mice were anesthetized and imaged (C) by Bruker Biospec 11.7T animal MR scanner, and the pH_{enh} was calculated and graphed (D). **(E)** p-TAK1, p-p65 and p-IKBa were increased in 4T1 cells under acidic conditions as shown by Western Blots. 4T1 cells were treated with HCl or NaOH to make pHe in a proper pH range (pHe= 6.50~8.30) for 12 hours. **(F, G)** The GM-CSF expression was upregulated in 4T1 cells under acidic conditions. 4T1 cells were treated with HCl or NaOH to make pHe in a proper pH range (pHe= 6.50~8.30) for 12 hours. GM-CSF mRNA expression was quantified by qRT PCR (B) and GM-CSF protein was measured in culture supernatant with ELISA (C). Data were presented as mean ± SEM, one-way ANOVA test was utilized; ns, no significance, *$p < 0.05$, **$p < 0.01$, ***$p < 0.001$.

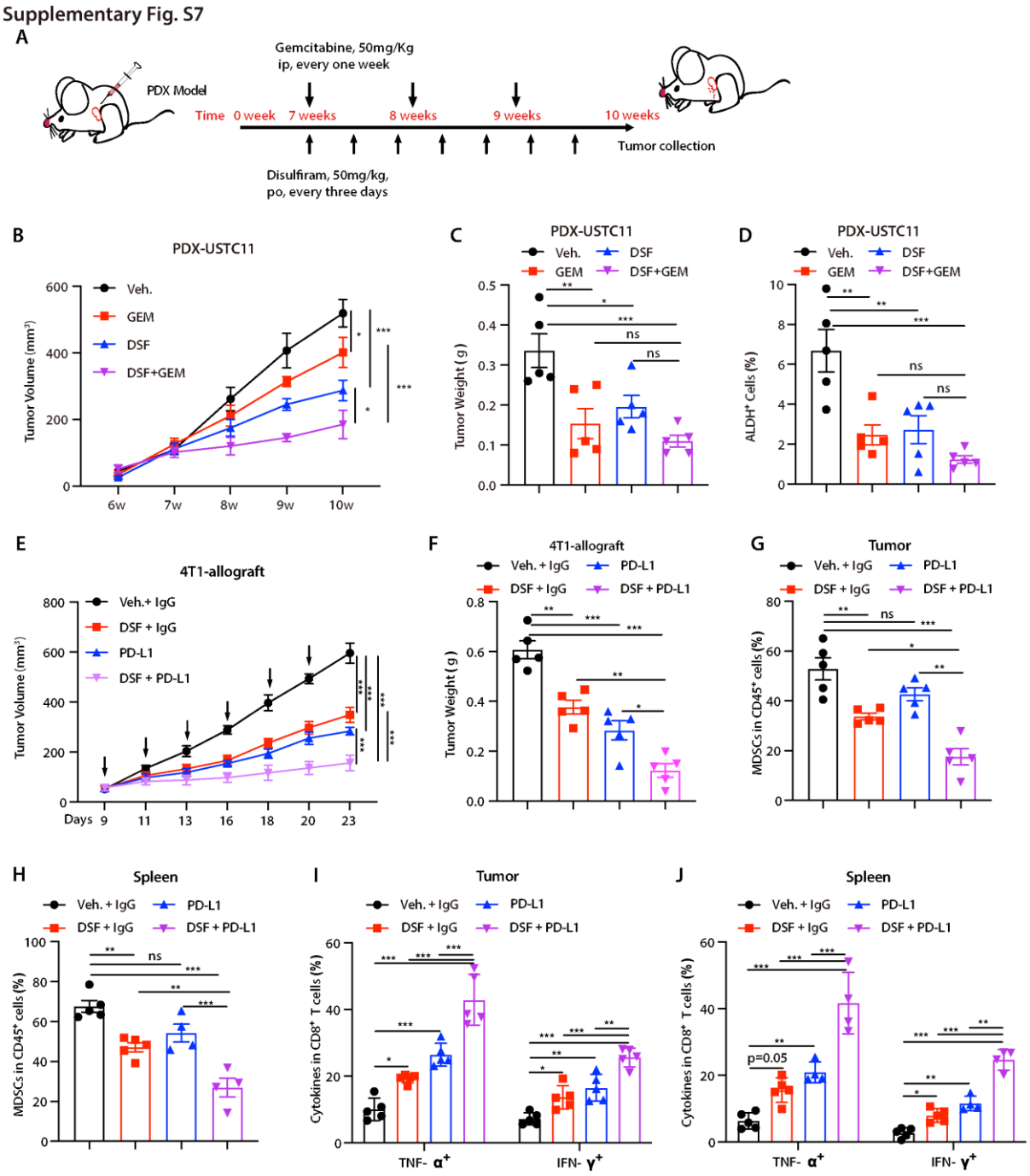

232

233 **Fig. S7. DSF enhanced the sensibility of the 4T1 tumors to GEM or PD-L1 antibody.**

234 **(A)** The experimental diagram for the combinational treatment. Tumor cells ($1x10^6$) digested

235 from PDX of TNBC (USTC11 established by our laboratory) were injected orthotopically

236 into NOD-SCID mice. When the average diameter of tumors reached to about 5mm, mice

237 were randomly divided into four groups and treated with Vehicle control, DSF (50mg/kg, po,

once every three days) and GEM (50mg/kg, ip, once a week) alone or in combination. **(B, C)** The PDX tumor growth was significantly inhibited by the treatment of DSF and GEM alone or in combination (n = 5/group). Tumor volume was monitored once a week, and tumors were weighted after mice were euthanized. **(D)** $ALDH^+$ BTICs were obviously decreased by the treatment of DSF and GEM alone or in combination (n=5/group). **(E, F)** The growth of 4T1 allografts was significantly inhibited by the treatment of DSF alone and PD-L1 antibody alone or in combination (n=5/group). 4T1 cells ($5x10^4$) were injected orthotopically into female Balb/c mice. After 9 days, mice bearing palpable tumors were randomly divided into four groups and treated with Vehicle control, DSF (50mg/kg, po, every 2-3 days as the arrow indicated) and PD-L1 antibody (200 ug/mice, ip, every 2-3 days as the arrow indicated) alone or in combination. **(G, H)** The proportion of $CD11b^+Gr1^+$ MDSCs in the tumors and spleens of control-, DSF-, PD-L1- and combination-treated mice were analyzed using flow cytometry (n=5/group). **(I, J)** The proportion of IFN-γ^+CD8^+ T cells and TNF-α^+ $CD8^+$ T cells were analyzed in tumors and host spleens after the treatment of DSF and PD-L1 antibody alone or in combination (n=5/group). Data were presented as mean ± SEM, one/two-way ANOVA test was utilized; ns, no significance, *$p < 0.05$, **$p < 0.01$, ***$p < 0.001$.

Supplementary Fig. S8

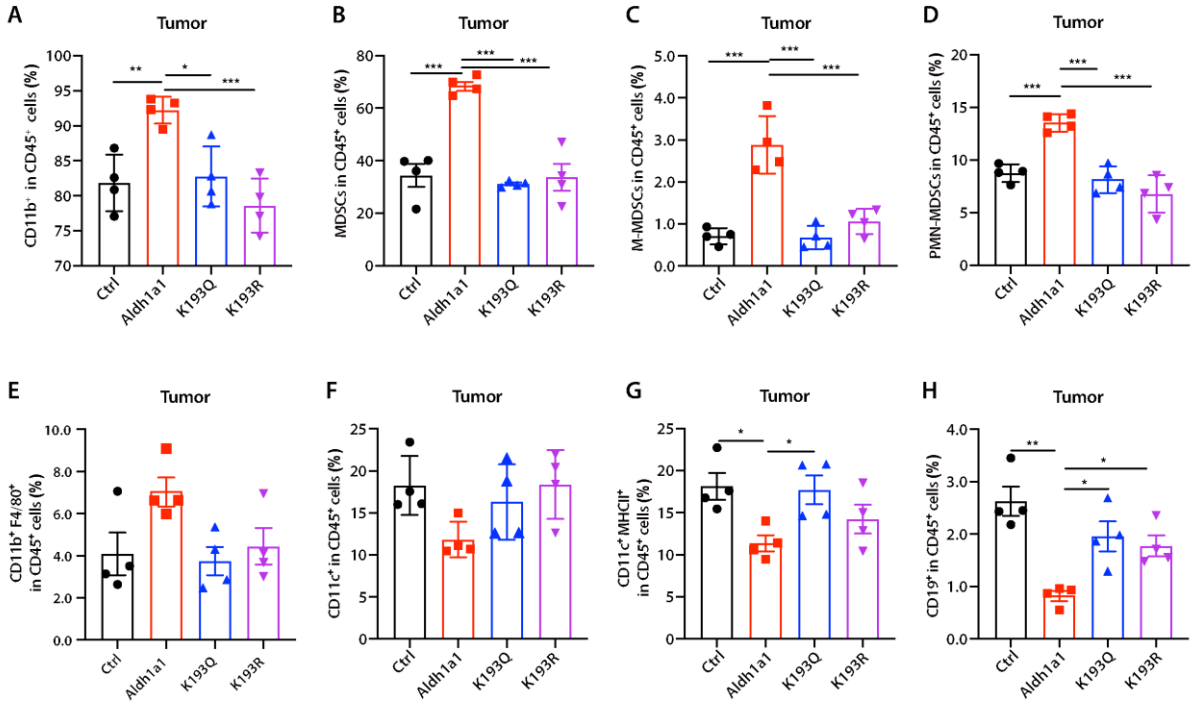

Fig. S8 Aldh1a1 altered the infiltration of TAMs, DCs and B cells in tumor microenvironment.

(A) Percentage (in $CD45^+$ cells) of $CD11b^+$ myeloid cells from control-, Aldh1a1-, K193Q- and K193R-4T1 tumors (n=4 /group). **(B)** Proportion (in $CD45^+$ cells) of $CD11b^+Gr1^+$ MDSCs from control-, Aldh1a1-, K193Q- and K193R-4T1 tumors (n=4 /group). **(C, D)** Proportion (in $CD45^+$ cells) of M-MDSCs and PMN-MDSCs in the tumors from control-, Aldh1a1-, K193Q- and K193R-4T1 tumors (n=4 /group). **(E)** Proportion (in $CD45^+$ cells) of $CD11b^+F4/80^+$ TAMs in the tumors of control-, Aldh1a1-, K193Q- and K193R-mice were analyzed using flow cytometry (n=4 /group). **(F)** Percentage (in $CD45^+$ cells) of $CD11c^+$ cells from control-, Aldh1a1-, K193Q- and K193R-4T1 tumors (n=4 /group). **(G)** Percentage (in $CD45^+$ cells) of $CD11c^+MHCII^+$ DC cells from control-, Aldh1a1-, K193Q- and K193R-4T1 tumors (n=4 /group). **(H)** Percentage (in $CD45^+$ cells) of $CD19^+$ B cells from control-, Aldh1a1-, K193Q- and K193R-4T1 tumors (n=4 /group). Data were presented as mean ± SEM, one-way ANOVA test was utilized; ns, no significance, *p < 0.05, **p < 0.01, ***p < 0.001.